South African Journal of Botany 186 (2025) 1–12

Contents lists available at ScienceDirect

South African Journal of Botany

journal homepage: www.elsevier.com/locate/sajb

Investigation of *Ximenia afra* Sond. var. *afra* L. as a source of antiplasmodial and trypanocidal phytochemicals through accelerated bioactivity guided isolation

Wiehan Rudolph [a], Lauren Webster [b,c], Cedric Graebin [b,c], Vinesh Maharaj [a,d,*]

[a] Biodiscovery Centre, Department of Chemistry, Faculty of Natural and Agricultural Sciences, University of Pretoria, Hatfield, Pretoria 0002, South Africa
[b] Drug Discovery Unit, School of Life Sciences, University of Dundee, Dow Street, Dundee, DD1 5EH, Scotland, UK
[c] Wellcome Centre for Anti-Infectives Research, School of Life Sciences, University of Dundee, Dow Street, Dundee, DD1 5EH, Scotland, UK
[d] Office of the Deputy Dean: Research and Postgraduate Studies, Natural and Agricultural Sciences Building, University of Pretoria, Hatfield, Pretoria 0002, South Africa

ARTICLE INFO

Edited by: Dr S.C. Pendota

Keywords:
Plasmodium falciparum
Human African trypanosomiasis
Natural product drug discovery
Ximenia afra
Flavonoid glycosides
Semi-preparative HPLC
Nuclear magnetic resonance spectroscopy
Biological activity

ABSTRACT

Ethnopharmacological relevance: Ximenia afra has been shown to be a potential source for antiprotozoal lead compounds based on its tentatively assigned phytochemistry or purely based on ethnomedicinal applications, where infusions of root, stem, and leaf mixtures, are often used for treating a wide range of parasitic ailments, including malaria and human African trypanosomiasis (HAT). Previous phytochemical analyses of extracts from the leaves showed high abundances of flavonoids and proanthocyanidins, and exhibited moderate to good activity against infections of *Plasmodium* sp.

Aim of the study: This study was designed to (i) Rapidly determine the bioactivity of the extract and seven corresponding fractions, from the crude extract of *X. afra* leaves and twigs, against both *P. falciparum* and *Trypanosoma brucei*; (ii) isolate and characterise the bioactive compound from these fractions; (iii) confirm the bioactivity of the isolated compound against *P. falciparum* and *T. b. brucei*.

Materials and methods: An extract and fractions were produced from the mixed stems and leaves of *X. afra*. A set of seven polarity-based fractions were produced from the extract and evaluated in an *in vitro* phenotypic screen against single strains of bloodstream form *P. falciparum* (3D7) and *T. b. brucei* (Lister strain 427). High resolution mass spectrometry analysis was done on the bioactive fractions, to tentatively identify the constituents. Guided by these phytochemical profiles and the antiprotozoal activity of the fractions, a single compound was selected for targeted isolation. Quercitrin was isolated by semi-preparative high performance liquid chromatography (HPLC) and fully characterised by accurate mass analysis and nuclear magnetic resonance spectroscopy (NMR). Biological assays were done to determine the antiplasmodial and trypanocidal activities of quercitrin.

Results: In vitro phenotypic screening of the extract and fractions showed the mid-polar fractions exhibited significant antiplasmodial and trypanocidal activity. Tentative chemical profiling showed one of the highly bioactive fractions contained one major compound, which was then isolated. Accurate mass and NMR analyses confirmed the structure of the isolated compound as quercitrin. It was found to be active against *P. falciparum* (3D7), with IC_{50} = 2.76 μM (n = 2). However, the activity of the compound was poor against *T. b. brucei* (strain 427) (19 % inhibition at 25 μM; n = 1) and showed no inhibitory activity in the *P. falciparum* lysyl tRNAse synthetase (*PfKRS1*) assay.

Abbreviations: HPLC, High performance liquid chromatography; UPLC-QTOF/MS, Ultra-high performance liquid chromatography-Quadrupole Time-of-flight Mass spectrometry; NMR, Nuclear Magnetic Resonance Spectroscopy; HAT, Human African trypanosomiasis; *Pf*KRS1, *P. falciparum* lysyl tRNAse synthetase; MMV, Medicines for Malaria Venture; WHO, World Health Organisation; ACT, Artemisinin combined therapy; CDC, U.S. Centres for Disease Control and Prevention; IKS, Indigenous knowledge systems; DCM, Dichloromethane; MeOH, Methanol; CQs, Chloroquine sensitive; CQr, Chloroquine resistant; SI, Selectivity Index; IC50, Concentration producing 50 % inhibitory effect; EtAc, Ethyl acetate; MTBE, tert-Methyl butyl ether; FA, Formic acid; SPE, Solid-phase extraction; BSF, Bloodstream form; DWP, Deep-well plate; PDA, Photodiode array detector; m/z, Mass-to-charge ratio; MoA, Mode of action; DDU, Drug Discovery Unit; WCAIR, Wellcome Centre for Anti-Infectives Research; UD, University of Dundee; UP, University of Pretoria.

* Corresponding author at: Office of the Deputy Dean: Research and Postgraduate Studies, Natural and Agricultural Sciences Building, University of Pretoria, Hatfield, Pretoria 0002, South Africa.

E-mail addresses: wiehan.rudolph1@gmail.com (W. Rudolph), l.a.webster@dundee.ac.uk (L. Webster), CGraebin001@dundee.ac.uk (C. Graebin), vinesh.maharaj@up.ac.za (V. Maharaj).

https://doi.org/10.1016/j.sajb.2025.08.037
Received 4 June 2025; Received in revised form 3 August 2025; Accepted 29 August 2025
Available online 5 September 2025

Conclusion: Further scientific evidence for the effectiveness of *X. afra*, in the treatment of malaria and HAT, was obtained. Quercitrin, for the first time, was isolated from the leaves and stems of *X. afra* and its activity against *P. falciparum* (3D7) was confirmed *in vitro* by phenotypic assay. Its activity against this strain was, until now, unknown. Although quercitrin alone was not a potent trypanocidal compound, the combination of it with other flavonoids and proanthocyanidins provided good activity (%-inhibition > 80 %).

1. Introduction

Malaria as a disease is well-documented and remains an ongoing global concern. Uncomplicated malaria is often mistaken for other infections, such as influenza (MMV, 2023b). Should the disease remain untreated, it will progress to severe malaria, a life-threatening condition with symptoms as described by the MMV's Severe Malaria Observatory (2025). *Plasmodium falciparum* (transmitted only by female mosquitoes of *Anopheles* spp.) is the most aggressive malaria species and is responsible for causing most of the severe malaria cases and associated mortalities in sub-Saharan Africa (MMV, 2023a). Depending on the severity of malaria in the infected individual, treatments may differ. The World Health Organisation (WHO, 2024) recommends oral artemisinin (and artemisinin derivative)-combined therapies (ACTs) for the treatment of uncomplicated malaria. For the treatment of severe malaria, intravenous artesunate is recommended (WHO, 2024).

An emerging challenge is the development of partial drug-resistance by *P. falciparum*, which has been attributed to mutations in the parasite's *kelch13* (*PfK13*) gene (Ndong Ngomo et al., 2023). Other key genes affected through parasite mutation were *Pfcrt*, and *Pfmdr2* which are associated with artemisinin resistance (Ndong Ngomo et al., 2023). Recent studies (Fola et al., 2023; Ndong Ngomo et al., 2023; Schmedes et al., 2021) have shown that partial drug-resistance is spreading rapidly throughout sub-Saharan Africa and central and east Asia.

Infections with *Trypanosoma brucei spp*., causing human African trypanosomiasis (HAT), are still being neglected (CDC, 2019). Among the different variants and subspecies of *T. brucei* spp., two species are capable of infecting humans: *T. b. rhodesiense* (East African HAT), and *T. b. gambiense* (West African HAT) (Gunn and Pitt, 2012; Ismail et al., 2020). East African HAT is very aggressive with a much higher morbidity rate than West African HAT, however, the West African variant is far more prevalent, being responsible for 92 % of trypanosomiasis cases (Kuepfer et al., 2011). Both parasites are transmitted by the tsetse flies of the genus *Glossina* (Gunn and Pitt, 2012; Ismail et al., 2020).

The U.S. Centres for Disease Control and Prevention (CDC) indicates both West and East African HAT develop through two stages of infection of the human host. The first stage of the disease is marked by swollen lymph nodes and malaise. Neurological symptoms, especially sleep cycle reversal and hallucinations, mark the onset of the second stage of disease. Over the last five years the burden of HAT has been eased significantly (CDC, 2020). Yet, as early as 2013, melarsoprol-resistance has been documented. Isolation of the *TbAT1* gene from resistant parasites showed mutations that prevented coding of the P2 adenosine transporter protein – a part of the uptake pathway for melarsoprol and other trypanocidal drugs (Baker et al., 2013; Nerima et al., 2007).

Throughout the African continent, *Ximenia afra* (illustrated in Fig. 1), colloquially known as the 'suurpruim' (afr.), or 'umthunduluka' (zul.), is used in ethnic medicine for various ailments (Hutchings et al., 1996; van Wyk and Gericke, 2018; Watt and Breyer-Brandwijk, 1962). The ethnomedicinal applications of *X. afra* correlate well with the symptoms of both malaria and first-stage HAT (Hutchings et al., 1996). A catalogue of common African medicinal plants also lists *X. afra* roots, leaves, and stems as remedies specifically for malaria and 'sleeping sickness' (HAT) (Iwu, 2014). The *in vitro* antiplasmodial activity of extracts from *X. afra* has been reported in an earlier study by Clarkson et al. (2004). Herein, the medium polar and broad-spectrum extracts (DCM and 1:1 DCM/MeOH) showed moderate activity with IC_{50} values of 43.5 µg/mL and 55 µg/mL, respectively (Clarkson et al., 2004). Yet, the active antiplasmodial and trypanocidal constituents in *X. afra* have not been isolated, making this study the first to assign antiplasmodial activity to a specific constituent of *X. afra*.

Fig. 1. (A) X. afra growing *in situ*. (B) A close-up of the fruit and aerial parts of X. afra – Sourced from Plants of the World Online (POWO) (2025).

Phytochemically, *X. afra* is considered diverse in its classes of constituents. A study by Jacob et al. (2021) has shown that the leaves are rich in compounds of the medium-polar classes, such as flavonoids, saponins, and tannins. Some alkaloids were also found to be present, during this study. Maroyi (2016) also found *p*-coumarins to be present in leaf extracts of *X. afra* as well as a bis-norsesquiterpenoid. These studies did not proceed with the isolation of the phytochemicals (Jacob et al., 2021; Maroyi, 2016). Furthermore, it was found that several extensive natural products databases (PubChem (2025), NPASS (Zong and Xian, 2023), LOTUS Natural Products Database (Rutz et al., 2022)) do not contain any phytochemicals linked directly to the species *X. afra*, nor to its former name *X. caffra* [*sic*].

The antiplasmodial properties of flavonoids were investigated by Soré et al. (2018). Their conclusion was that flavonoids, due to low micromolar antiplasmodial activity (IC_{50} < 10 µM) against chloroquine-sensitive (CQs) and -resistant (CQr) strains, may hold the key to unlocking new antiplasmodial drugs. Additionally, in 2006 a study found that several phytochemicals of the flavonoid, flavanoid, and coumarin classes show strong-moderate trypanocidal activity with IC_{50}s in the low micromolar range (Tasdemir et al., 2006). Larit et al. (2021) have also found that some flavonoids exhibit activity against *T. brucei* parasites with potencies comparable to the commercial trypanocidal drug, eflornithine. In addition to the reported ethnomedicinal use of *X. afra* in the treatment of HAT, the expected presence of flavonoids, flavanoids, and coumarins therein also provides rationale for investigating the trypanocidal activity of its phytochemicals.

2. Materials and methods

2.1. Chemicals – reagents and solvents

For the extraction of plant material, dichloromethane (DCM, UnivAR®-grade) and methanol (MeOH, UnivAR-grade) were purchased from Merck (Pty) Ltd. In the fractionation of the extracts, the following solvents were used: de-ionised water (dH_2O, resistance of 18.2 MΩ, from an Elga Chorus Purelab water purification system, from Labotec (Pty) Ltd), methanol 215 (MeOH, ROMIL SpS-grade) and acetonitrile 200 (ACN, ROMIL SpS-grade) from Microsep (Pty) Ltd, ethyl acetate (EtAc, for HPLC, >99.7 %) from Merck (Pty) Ltd, and tert-butyl methyl ether (MTBE, for HPLC, >99.8 %), also from Merck (Pty) Ltd. For sample sub-zero storage medium, dimethylsulfoxide (DMSO, for molecular biology) was purchased from Merck (Pty) Ltd.

Mobile phases and solvents for sample preparation in semi-

preparative HPLC-UV-MS were composed of methanol 215 and acetonitrile 200 (SpS-grade, ROMIL), and dH_2O (as used for fractionation). For semi-prep-HPLC the mobile phase solvents were spiked with formic acid (FA) (LC-MS grade, Fischer Chemical), purchased from LabChem (Pty) Ltd to 0.1 % v/v. These solvents were also used in the sample preparation for UPLC-qTOF/MS analysis. Mobile phases for UPLC-QTOF/MS consisted of UpS-grade MeOH and ACN, purchased from Microsep (Pty) Ltd, and dH_2O (as used for fractionation). All three these solvents were buffered to contain 0.1 % (v/v) FA (99+ %, Thermo-Scientific), purchased from LTC Technology (Pty) Ltd.

For NMR analyses, deuterated methanol (methanol-d4 CD_3OD, 99.8 atom %-D) was purchased from Merck (Pty) Ltd.

2.2. Sourcing of plant material

Ground dry stems and leaves of *X. afra* was sourced from the in-house Biodiscovery repository of plant material, catalogued as P25486. The original collection of the material was done by the Council for Scientific and Industrial Research (CSIR) from the Blyde River Canyon grasslands in Mpumalanga, South Africa (GPS coordinates: 24°32′39.4″S; 30°47′31.6″E). A voucher specimen for the original collected material is housed at the South African National Biodiversity Institute's (SANBI) herbarium in Pretoria under the field collection number JM00260 and accession number PRE0894208–0.

2.3. Extraction of plant material

The high-throughput system used by the Biodiscovery Centre, for plant extraction and extract fractionation, was developed based on the approach used by the National Cancer Institute in the USA (Thornburg et al., 2018). The approach aims to reduce the time and resources required to make an informed decision on the selection of plants for a study on Natural Products Drug Discovery.

For the extraction, 7.02 g of dry plant material was transferred into an extraction tube with a grade-3 sintered glass disc as filter. This tube was then topped off with 50.0 mL of a 1:1 methanol/dichloromethane (MeOH/DCM; UnivAR®-grade) solvent system, and sonicated for one hour at 25 to 40 °C. The extract was collected by positive-pressure filtration through the sintered glass disc of the tube.

A second extraction step was performed on the material by sonication in 50.0 mL MeOH (UnivAR-grade) for one hour. The second extract was combined with the first and up-concentrated by rotary evaporation (R-300 Rotavap, Büchi from Labotec (Pty) Ltd) at a temperature of 35 °C. Complete drying was achieved in a Genevac® EZ-2.3 Plus (SP Scientific via United Scientific (Pty) Ltd) centrifugal evaporator at 35 °C.

2.4. Fractionation of extracts and high-density storage of extract and fractions

A portion of the extract obtained (251.6 mg) was reconstituted in 4.36102 mL of 6:3:1 MeOH/EtAc/MTBE. Of this, a small volume (96.2 µL) was transferred to a 96 deep-well plate (DWP, BioPointe) for storage in the Biodiscovery Centre library. This liquid handling was performed on a Hamilton Microlab STARLet liquid handler (Separations (Pty) Ltd). The remainder of the reconstituted extract was adsorbed onto a roll of cotton wool (TIDI, CC Immelman (Pty) Ltd) and dried in *An sp* Scientific Genevac HT-6 Series 3i (United Scientific (Pty) Ltd) centrifugal evaporator.

Fractionation of a portion of the extract (251.60 mg) was performed by automated solid-phase extraction (SPE) on HyperSep C8 reverse phase cartridges (6 mL, 2 mg sorbent, ThermoFisher via Anatech (Pty) Ltd). Automated liquid handling, in this step, was done on a Gilson GX-241 ASPEC coupled to a Verity 4060 liquid pump. The cartridge was conditioned with 20 mL MeOH and equilibrated with the first of seven solvent systems (95 % dH_2O/5 % MeOH-215, 20 mL). The adsorbed extract was loaded in an empty Phenomenex 6 mL SPE-cartridge (Separations (Pty) Ltd) and connected on top of the C8-cartridge with a PTFE adapter.

The combined cartridge was eluted with a series of seven eluents of decreasing polarity (dH_2O/MeOH): (1) 95:5, (2) 8:2, (3) 6:4, (4) 4:6, (5) 2:8, (6) 0:100, (7) MeOH/ACN 1:1. At each step 9.0 mL of solvent was passed through the combined cartridge and the eluate collected as seven individual fractions. Of each fraction a 1.600 mL aliquot was transferred to the same library DWP. Both the plate and the remaining fraction material collected, were dried in a Genevac HT-6 Series 3i centrifugal evaporator. Based on the mass of fraction material calculated to be in each well in the plate, the dried aliquots and extract were reconstituted in DMSO and standardised to a concentration of 5 mg/mL. These samples were transferred to 1 mL FluidX-tubes (Separations (Pty) Ltd) stored at −20 °C in a Hamilton Storage Verso Q20 robotic freezer.

For export of the samples, the FluidX-tubes were retrieved and aliquoted to a NEST 96 deep-well plate (Lasec SA (Pty) Ltd), with the aid of the STARLet microlab. The 96-DWP was heat sealed with an aluminium seal for transport to the Wellcome Centre for Anti-Infectives Research (WCAIR), at the University of Dundee (UD).

2.5. In vitro screening of samples against P. falciparum

2.5.1. Phenotypic single-point screening

In this study, the samples were screened against the widely used 3D7 chloroquine sensitive (CQs) strain of *P. falciparum* (3D7) in its asexual blood-stage form (BSF). Screening was done according to the standard method used at the WCAIR/UD Drug Discovery Unit (DDU), as described in the supplementary information to their study on the antimalarial activity of trisubstituted pyrimidines (Norcross et al., 2016). In short, the *P. falciparum* (3D7) cultures were maintained in a 5 % suspension of human red blood cells (RBCs), obtained via from the East of Scotland Blood Transfusion Service at Ninewells Hospital (Dundee, Scotland). Prior to introduction to the human RBC suspension, the cultures were developed in RPMI 1640 medium, with the pH maintained at 7.3 (Norcross et al., 2016).

Samples were screened in duplicate ($n = 2$) at a final concentration of 2.5 µg/mL in culture. Potency of sample extracts, fractions, and compounds were measured by fluorescent assay in monitoring the binding of SYBR green dye to double stranded DNA in the assay samples. Mefloquine, a potent commercial, antiplasmodial drug for treating severe malaria, was used as positive control with a potency range of 30–60 nM (Norcross et al., 2016).

An IC_{50} was estimated for the isolated compound by following the same phenotypic screening against *Pf*3D7, but at nine logarithmically spaced compound concentrations of 1 nM to 25 µM, to generate a dose-response model, in duplicate ($n = 2$). From the equation of the curve, the IC_{50} was calculated by interpolation.

2.5.2. Enzymatic assay for estimation of PFKRS1 activity

A mode-of-action (MoA) investigative study, for inhibition of *P. falciparum* lysyl-tRNA-synthetase (*Pf*KRS1), was done with the isolated compound. The *in vitro* enzymatic assay was done, as described by Baragaña et al. (2019), in a final volume of 50 µL. The compound of interest and enzyme were added to give a final concentration of 7.5 µM and 8.1 nM of *Pf*KRS1, respectively, in the buffered medium. A 2 µM solution of adenosine triphosphate (ATP) was used to initiate the enzymatic reaction, which proceeded under 30 °C incubation for 180 min, while shaking at 90 rpm. This reaction was terminated with the addition of 50 µL of Kinase-Glo reagent (Promega, Madison, Wisconsin). The reaction mixtures were analysed on a PerkinElmer MicroBeta2 plate reader (Waltham, Massachusetts).

2.6. Screening of samples against T. b. brucei

In this study trypanocidal activity was measured as inhibition of *T. b. brucei* parasites. This non-human infective strain was used as it shares

genetic similarity to the human infective subspecies (*T. b. gambiense* and *T. b. rhodesiense*) but is also more readily available and safer to use in higher throughput screening. It is also monomorphic with stable genetic sequences, making it suitable for wider applications at the WCAIR. (Peacock et al., 2008)

2.6.1. Phenotypic single-point screening

Screening for trypanocidal activity in the extract and fractions was done as a single-point phenotypic assay, without replication, at the DDU in Dundee (UK). For the assay, trypomastigotes of *T. b. brucei* (Lister strain 427) were cultured in a modified HMI9 medium, where 200 μM 2-mercaptoethanol was used as per Frearson et al. (2010). Culturing was done at 37 °C and monitored by haemocytometry. A two-colour assay was used to confirm cell viability of the cultures, pre-screening. With appropriate dilutions, 200 μL of the *T. b. brucei* (strain 427) culture (10^4 cells/mL) were transferred to wells in a 96-well plate, after each well was first spiked with 1 μL of the test sample (extract or fraction solubilised in DMSO), giving a final concentration of 12.5 μg/mL extract or fraction per well. One column of the 96-well plate was kept unspiked with cell culture and was spiked only with media and DMSO as a reference. The assay plate was incubated for 69 h at 37 °C under a 5 % CO_2 atmosphere (Frearson et al., 2010).

Visualisation of the trypanosomes, for quantification by fluorescence, was done by spiking each sample well of the assay plates with 20 μL resazurin, having a final in well concentration of 50 μM, and further incubating the plates for four hours. After this incubation period, the well fluorescence was measured using a BioTek flx800 plate reader, set to monitor λ(excitation) = 528 nm and λ(emission) = 590 nm (Frearson et al., 2010). As positive control melarsoprol, at a final in-well concentration of 5 μM, was used to induce a 100 % effect on trypanosomes.

2.6.2. Nine-point duplicate screening for IC_{50} calculation

For the estimation of the IC_{50} of the isolated compound, the assay was performed in duplicate ($n = 2$) on the same concentration range as was used for the estimation of the antiplasmodial IC_{50}. The data allowed for the estimation of the dose-response curve of the isolated compound (s) and, thereby, its IC_{50}.

2.7. UPLC- QTOF/MS analysis of active fractions and extract

Following the screening of the extract and fractions, the active fractions and the extract were analysed by UPLC-QTOF/MS to generate tentative phytochemical profiles, using a Waters UPLC-system, hyphenated with Waters SYNAPT G2 HRMS QTOF mass analyser. Samples were introduced via a Waters Aquity Sample Manager and the mobile phase managed by a Waters Aquity BSM module. The sample injection volume was set to 5.00 μL. Accurate mass analysis was done relative to a leucine enkephalin LockSpray internal standard (target at m/z(ESI+) = 556.2771 and m/z(ESI-) = 554.2615). The instrument achieved a full width-half maximum (FWHM) mass resolution of 18 000 in both ionisation modes.

Separation of compounds was accomplished on an Aquity UPLC BEH C18 column (2.1 × 100 mm; 1.7 μm particle diameter), with a gradient H_2O/MeOH (both buffered to 0.1 % v/v formic acid (FA)) solvent system. The method started at 97 % H_2O/3 % MeOH with a flow rate of 0.3 mL/min. Initial conditions were maintained for 0.10 min, followed by a linear increase in the %-MeOH to 100 %, at 14.00 min. This was maintained for 2.00 min, whereafter the system was changed back to initial starting conditions over 0.50 min at a linear gradient. The column was equilibrated at these conditions for 3.50 min before the next run, giving a total runtime of 20.00 min. Throughout the run the column temperature was kept at 50 °C. The instrument was controlled via MassLynx™ v4.1.

Analysis of the eluting compounds was done in the positive and negative ES-ionisation (ESI) modes. In both the positive and negative ESI-modes, a mass range of 50 to 1200 mDa was set. Tentative identification of the active fraction profile constituents was done on MassLynx v4.2 and the UNIFI™ application manager (version 3.6.0.21) on the Waters_Connect Informatics Platform version 7.1.0 (Wilmslow, Manchester). Manual annotation via MassLynx was accomplished by comparing calculated chemical formulas to compounds known to occur in plants of the family Olacaceae. Either reported in published data (Maluleke et al., 2024; Zhen et al., 2015), or in databases such as LOTUS: Natural Products Online (Rutz et al., 2022) and the NIH's PubChem Database (Kim et al., 2023). Annotation via UNIFI was done through the built-in Waters Traditional Medicine Library.

2.8. Repeated extraction and targeted fractionation

In setting up for the isolation of constituents in the active fractions, 32.52 g of the same plant sample used initially, was extracted three times for 24 h in a 1:1 DCM/MeOH (UnivAR, 350 mL) solvent system, with agitation on an FMH orbital shaker bed at 180 rpm. The extracts were combined and dried by rotary evaporation on a Büchi R-300 Rotavap. Of this extract 2.0695 g was weighed out and solubilised in 10 mL 80 % dH_2O/20 % MeOH (SpS-grade, ROMIL). Three fractions were generated by manual fractionation on a HyperSep C8 SPE cartridge (6 mL, 2 mg sorbent): (dH_2O/MeOH) (U1) 8:2, (U2) 4:6, (U3) 2:8.

2.9. Isolation of suspect leads by semi-preparative HPLC-UV/MS

Based on correlation between the UPLC-QTOF/MS chromatograms of the active fraction and the three upscaled fractions, the one containing the most of the active fraction constituents was selected for isolation of compounds by semi-preparative HPLC-UV/MS. In this system a Waters 2545 Binary Gradient Module, a Waters 2767 Sample Manager, and a Waters System Fluidics Organizer (SFO) were used to introduce the sample and mobile phases. Analysis of the target fraction, prior to isolation, was done on a 4.6 × 150 mm C18 column. Compound isolation was done on an XBridge BEH C18 OBD semi-preparative column (10 × 150 mm, 5 μm particle diameter) and a 2 mL injection loop (200.00 μL injection volume). Eluting compounds were detected by in-line UV-analysis, on a Waters 2998 PDA detector, and an Aquity QDa mass detector. Instrument control and data analysis was done on MassLynx v4.1.

For the fraction analysis, preceding isolation, a flow rate of 1.00 mL/min was applied with a gradient solvent system starting from 95 % H_2O/5 % MeOH (0.1 % v/v FA) held for 0.10 min. A linear gradient was applied to change the composition to 100 % MeOH over 13.90 min. This mobile phase composition was maintained for two minutes, after which it was reverted to the starting composition in 0.50 min. To equilibrate the column for the next analytical run, the mobile phase composition was maintained at 95 % H_2O/5 % MeOH for 3.50 min.

Elution of samples through the semi-preparative column was again accomplished with a H_2O/MeOH (0.1 % v/v FA) solvent system, starting at 95 % H_2O/5 % MeOH, held for 0.10 min and then ramped, linearly over 16.90 min, to 100 % MeOH. The system was kept at this composition for 3.00 min and then changed back to the 95 % H_2O/5 % MeOH starting composition, at a linear rate over 0.50 min. To equilibrate the column for the next run, this setting was maintained for 3.50 min. A flow rate of 5mL/min was use throughout the run time.

Fraction collection was done based on a "timed events" collection method, programmed in the FractionLynx suite in MassLynx. The retention time range, for collection, was set by observing the elution of the target compound in a trial run on the semi-prep system. To allow for fraction collection in parallel with sample analysis, a 1 000:1 splitter module and Waters 515 HPLC make-up pump was used. The former splits 1 000 parts of the flow from the semi-prep column to the Sample Manager, for fraction collection, and one part to the PDA and QDa-spectrometers, with the aid of the Waters 515 make-up pump (0.50 mL/min MeOH with 0.1 % v/v FA) to generate a 0.5 mL/min flow rate into the QDa-ion source.

UV-analysis was done over the range 215 to 400 nm. Semi-preparative HPLC-runs were done with the MS set to the negative ESI-mode. The MS was allowed to scan, with nominal mass resolution, over a range of 100 to 1 000 Da.

2.9.1. UPLC-QTOF/MS analysis of upscaled fractions and isolated compound

Analyses of the semi-pure fraction and pure compounds via UPLC-QTOF/MS was done with the same system and gradient method as the analyses of the extracts and small scale SPE fractions.

2.10. NMR-analysis of an isolated compound

NMR-analyses were done with a Bruker Ascend 500 MHz cryo-probe spectrometer, coupled to a Bruker SAMPLECASE autosampler and an AVANCE III HD spectrometer processor, and operated via Bruker TopSpin 3.7.0. Sample preparation was done in a 5 mm Norell NMR tube (for 500 MHz conditions, Merck (Pty) Ltd). Methanol-d4 (CD_3OD, section 2.1) was used to solubilise the sample for NMR analysis. Data analysis was done on the Bruker TopSpin 4.1.4 software suite, under an academic license. For full characterisation of isolated compounds, the following experiments were run: (1D) ^{1H}NMR , ^{13C}NMR , and (2D) HSQC-DEPT, HMBC, COSY and NOESY.

3. Results and discussion

3.1. Extraction and fractionation of X. afra

Extraction of the 7.02 g, of dry leaves and stems from *X. afra*, yielded 808.16 mg (11.5 % m/m) dry extract, referenced as P25486xe8. Automated fractionation of P25486xe8 (251.60 mg) produced seven fractions (P25486xf1–7) with yields as shown in Table 1.

3.2. Screening of extract and fractions against P. falciparum

Initial single point screening (n = 2) of the samples, against *P. falciparum* 3D7, showed excellent inter-sample selectivity with only specific fractions showing potential for containing potent antiplasmodial compounds as depicted in Fig. 2. The extract of *X. afra* (P25486xe8) showed moderate activity with 96.9 (±SD = 0.1) % inhibitory effect. Antiplasmodial activity in the fraction followed a symmetrical distribution and was at a maximum in the medium-polar fractions (fractions 3 and 4), showing antiplasmodial activity with %-inhibitory effects (±SD) of 108.6 (±1.8) % and 105.1 (±2.2) %, respectively. Moderate activity (%-inhibition between 80 % and 100 %) was observed for fractions 2 (83.6 (±2.0) %) and 5 (93.4 (±0.1) %). Weaker activity was observed for fraction 6 (53.6 (±6.4) %), with fraction 1 the weakest (39.6 (±14.2) %). Since the samples were screened at approximately 25 µg/mL, the activity of the fractions was classified as moderate to good per Vergara, et al.'s (2022) reference to WHO antiplasmodial activity classification. Notably, fraction 7 was not assayed due to insufficient sample volume for a complete assay experiment.

In comparison to the study by Clarkson et al. (2004), this observed trend in antiplasmodial activity is not unexpected. In both this study, and that of Clarkson et al. (2004), the medium-polar phytochemicals appear to be the causative constituents for activity against *P. falciparum*. The close correlation between the DCM/MeOH (1:1) extract and medium polar fractions, in this study, also closely resembles the previously reported activity thereof (Clarkson et al., 2004). Since the combined mass yields of fractions 3 and 4 account for the largest partition of the extract by mass, it is likely these medium polar constituents account for most of the antiplasmodial activity observed.

Table 1
Yields from the automated fractionation of P25486xe8.

Fraction	Mass (mg)	%-Yield (from 251.60 mg extract)
P25486xf1	55.11	21.90 %
P25486xf2	23.12	9.19 %
P25486xf3	38.97	15.49 %
P25486xf4	44.38	17.64 %
P25486xf5	12.07	4.80 %
P25486xf6	7.53	2.99 %
P25486xf7	6.05	2.40 %

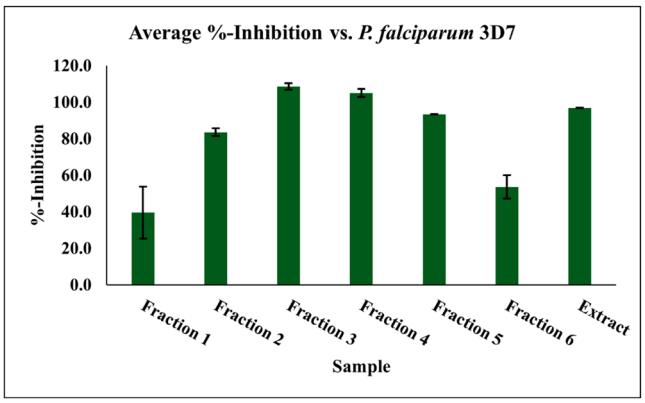

Fig. 2. Bar graph showing the average %-inhibitory effect of the extract and each fraction against P. falciparum (3D7). The error bars display one standard deviation from the mean (n = 2).

The variance in the data was evaluated through single factor ANOVA, grouped by screening replicates performed. A 95 % confidence level (α = 0.05) was applied to the analysis. As can be seen from the resulting data, in Table 2, the resulting p-value was greater than α = 0.05 implying the variation between the two screening experiments was not significantly greater than the variation within the individual batches. This also shows the good repeatability of the experiment.

To determine whether the variation between the extract and fraction samples' bioactivities is significant, the data was grouped per sample and analysed by single factor ANOVA with α = 0.05. The results for this are given in Table 3. In this analysis the calculated p-value was less than α, indicating the variation between the samples screened was significantly greater than the variation between replicate screening experiments per sample. Since this analysis included the extract and the six fractions that were screened against *P. falciparum* (3D7), this ANOVA indicates the presence of distinct phytochemicals in individual fractions do not share equal antiplasmodial activity. This supports the step of fractionating extracts prior to biological assay as it provides less-complex samples with distinct biological activity – thereby significantly easing the task of targeting specific compounds for isolation.

3.3. Rapid screening of extract and fractions against T. b. brucei

Similar to that of the antiplasmodial screening, the trypanocidal activity was concentrated in the medium-polar fractions (fractions 2 to 4) with fraction 1 showing low activity (54.0 %). Trypanocidal activity in fractions 5 and 6 was comparable to what was observed against *P. falciparum* 3D7 (in this case 34.0 % and 98.1 % respectively). It was also observed that the extract (93.4 % inhibitory effect) and medium polar fractions were of similar potency. It is likely that the observed activity in the extract is largely due to the constituents of the same set of medium polar phytochemicals in the antiplasmodial fractions. Nevertheless, the distribution of trypanocidal activity between fractions 2 (99.2 %), 3 (92.8 %) and 4 (94.7 %), compared to neighbouring fractions (fractions 1 and 5), indicated which fractions potentially contained trypanocidal compounds. Fig. 3.

The correlation between the activity profiles, for the antiplasmodial and trypanocidal fractions and extracts, guided the selection of fractions 3 to 5 for further analysis by UPLC-QTOF/MS to generate a tentative

Table 2
Results from ANOVA-calculation for P. falciparum data, grouped by replicate experiment results.

Source of Variation	Sum of squares	Deg. of freedom	Mean sum of squares	Calculated *F*-value	*p*-value*	*F*-critical
Between replicates	72.80	1	72.80	0.10	0.75	4.75
Within replicate experiments	8562.63	12	713.55			
Total	8635.43	13				

* $\alpha = 0.05$.

Table 3
Results from ANOVA-calculation for P. falciparum data, grouped by sample screened.

Source of Variation	Sum of squares	Deg. of freedom	Mean sum of squares	Calculated *F*-value	*p*-value*	*F*-critical
Between samples screened	8380.80	6	1396.80	38.40	5.20×10^{-5}	3.87
Within samples screened	254.63	7	36.38			
Total	8635.43	13				

* $\alpha = 0.05$.

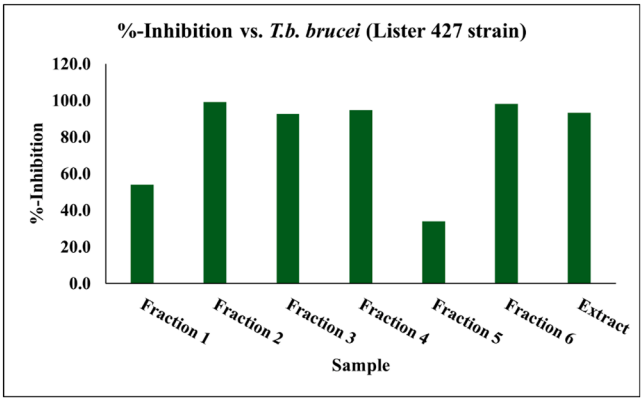

Fig. 3. A bar graph representation of the %-inhibitory effect of the extract and fractions from X. afra against T.b. brucei, *in vitro*. The experiment was done without replication ($n = 1$).

phytochemical profile of potential bioactives.

3.4. UPLC-QTOF/MS analysis of selected active fractions from X. afra

As expected from the broad-spectrum generic tests, performed by Jacob et al. (2021), the targeted medium polar fractions (no.'s 3 to 5) were found to contain mostly compounds of the flavonoid and proanthocyanidin type. The tentative annotations of these fractions are given in Table 4 and a broad spectrum overview of phytochemical class distribution over the seven fractions in fig.//. The majority of these tentatively identified compounds were localised in fraction 3. These compounds almost exclusively fall in the classes of proanthocyanidins and flavonols, apart from a simple benzyl glycoside and a linear diarylheptanoid. Fraction 4 showed significant overlap with both fractions 3 and 5, with all the tentatively annotated compounds therein also occurring in either fraction 3 or 5. As observed in fraction 3, the tentatively identified compounds in fractions 4 and 5 were mostly of the extended classes of proanthocyanidins and flavonoids. Fig. 4.

Of primary interest was the less complex and highly active (>90 % inhibitory effect *vs. P. falciparum* 3D7) fraction 5, consisting of a major compound with three minor compounds, as shown in Fig. 5B Since its major constituent, tentatively identified as quercitrin (1), was also present as a major compound in fraction 4, shown in Fig. 5A, it was considered to also be a potential moderately trypanocidal constituent. Guided by the antiplasmodial and trypanocidal activity in fractions 4 and 5, this major constituent of fraction 5 was targeted for isolation by SPE and subsequent semi-preparative HPLC fractionation.

The simplicity of fraction 5 and its potency shows the value of screening fractions *vs.* screening extracts. The rapid identification of individual potential targets for isolation, from the less complex fractions, is easily accomplished. Fractionation along a polarity gradient also provided good groupings of phytochemical classes, based on polarity. Based on the tentative identifications assigned, as per Table 4, the procyanidin derivatives were more localised in fraction 3. In contrast, the flavonol glycosides were more localised in fractions 4 and 5. The distribution of bioactivity across these fractions show how these different class groupings each contribute to the antiplasmodial and trypanocidal activity of the extract.

Compounds of the flavonoid and proanthocyanidin classes are well studied, but only recently attention has been given to their potential as new sources of antiplasmodial and trypanocidal drugs. Reviews by Fotie (2008) and Boniface and Ferreira (2019) indicated that several flavonoids have been found to exhibit moderate antiplasmodial activity ($IC_{50} < 20$ μM). In literature, quercetin has also been screened and found to be comparably trypanocidal to eflornithine, a commercial trypanocidal drug (Larit et al., 2021). In addition to quercetin, the reviews indicate several other flavonoid aglycones and glycosides as being moderately trypanocidal, including kaempferol.

Compound **(1)**, tentatively identified as quercitrin in fractions four and five, is a glycoside derivative of quercetin (quercetin-3-*O*-rhamnoside). Initial indications were, therefore that it should show at least similar levels of antiplasmodial and trypanocidal activity. Review of the literature showed that quercitrin has previously been screened for antiplasmodial activity against several strains. These results are listed in Table 5.

The data that has already been recorded for the activity of quercitrin against the *P. falciparum* 3D7 strain provides an opportunity for further investigations as these reported values are contradictory and not, necessarily, obtained via the same assay methods. Considering the simplicity of fraction 5, the results obtained for the antiplasmodial activity of quercitrin **(1)**, in this study, also contradict some of the findings in literature. This was further shown by obtaining the IC_{50} of quercitrin **(1)** *in vitro*, after isolating it and confirming its identity by chemical characterisation in the following sections.

3.5. Re-extraction and subsequent targeted SPE fractionation

The re-extraction of *X. afra* gave a total yield of 4.16 g (12.8 % m/m) of dried extract from 32.52 g dry plant material (plant material internal catalogue reference no. P25486). This was similar to the %-yield from the small-scale extract performed in the earlier experiment (see Section 3.1). Targeted fractionation, of a portion (2.0695 g) of this freshly prepared extract, was performed on SPE through elution with a stepwise gradient of decreasing %-H_2O in MeOH. This produced three fractions of high to low polarity: (U1 – 80 % H_2O) 448.22 mg (21.7 % m/m), (U2 – 40 % H_2O) 442.51 mg (21.4 % m/m), (U3 – 20 % H_2O) 32.98

Table 4
Tentatively identified constituents in fractions 3 to 5, as per recorded accurate mass data from UPLC-QTOF/MS analysis of these fractions. This tentative profile shows the simplicity of the highly bio-active fraction 5, from which its major constituent, quercitrin **(1)**, was isolated by semi-preparative HPLC.

Ret. time (min)	Observed *m/z* [Ion]*	Calculated *m/z* [Ion]	Compound name	Chemical formula	Fraction #	Tentative chemical structure
3.070	577.1333 $[M\text{-}H]^-$	577.1346 $[M\text{-}H]^-$	Kaempferol-7-*O*-(2-*E*-*p*-coumaroyl-α-*L*-rhamnopyranoside) **(2)**	$C_{30}H_{26}O_{12}$	3	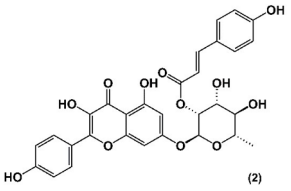 (2)
3.196	495.0803 $[M\text{-}H\text{+}FA]^-$	495.0780 $[M\text{-}H\text{+}FA]^-$	Myricetin-3-xyloside **(3)**	$C_{20}H_{18}O_{12}$	3	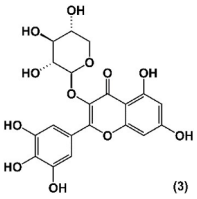 (3)
3.475	495.0807 $[M\text{-}H\text{+}FA]^-$	495.0780 $[M\text{-}H\text{+}FA]^-$	Hibiscetin-3-*O*-glucoside **(4)**	$C_{20}H_{18}O_{12}$	3	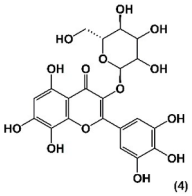 (4)
3.718	577.1334 $[M\text{-}H]^-$	577.1346 $[M\text{-}H]^-$	Procyanidin B1-B5 or B8 **(5)-(10)**	$C_{30}H_{26}O_{12}$	3	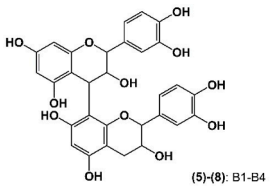 **(5)-(8)**: B1-B4 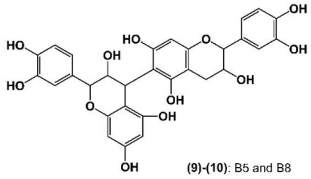 **(9)-(10)**: B5 and B8
3.877	729.1375 $[M\text{-}H]^-$	729.1461 $[M\text{-}H]^-$	Procyanidin B1–3-*O*-gallate **(11)**	$C_{37}H_{30}O_{16}$	3	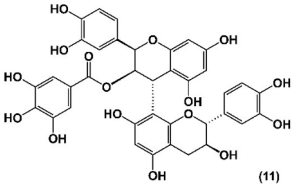 (11)
4.058	729.1383 $[M\text{-}H]^-$	729.1461 $[M\text{-}H]^-$	Procyanidin B3–3-*O*-gallate **(12)**	$C_{37}H_{30}O_{16}$	3,4	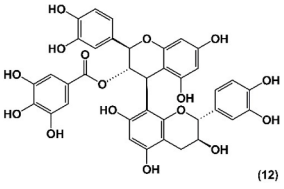 (12)
4.196	577.1323 $[M\text{-}H]^-$	577.1346 $[M\text{-}H]^-$	Apigenin-7-*O*-(6″-*E*-p-coumaroyl)-β-*D*-galactopyranoside **(13)**	$C_{30}H_{26}O_{12}$	3	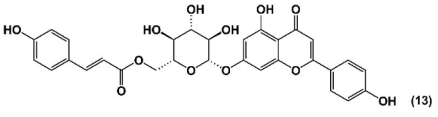 (13)

(*continued on next page*)

Table 4 (*continued*)

Ret. time (min)	Observed *m/z* [Ion]*	Calculated *m/z* [Ion]	Compound name	Chemical formula	Fraction #	Tentative chemical structure
4.344	881.1420 [M-H]⁻	881.1929 [M-H]⁻	Hydroxylated procyanidin C1 **(14)**	$C_{45}H_{38}O_{19}$	3,4	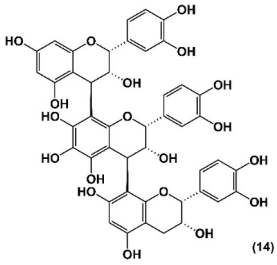 (14)
4.739	401.1496 [M-H]⁻	401.1448 [M-H]⁻	Benzyl-β-primeveroside **(15)**	$C_{18}H_{26}O_{10}$	3	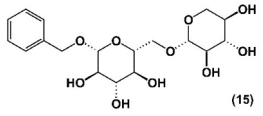 (15)
5.014	441.0867 [M-H]⁻	441.0822 [M-H]⁻	Catechin-*O*-gallate **(16)**	$C_{22}H_{18}O_{10}$	3,4	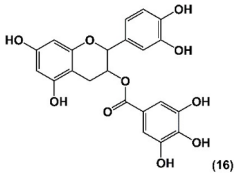 (16)
5.524	381.1812 [M-H]⁻	381.1854 [M-H]⁻	1,7-diphenyl-4-(2-phenylethyl) hept-1-ene-3,5-dione **(17)**	$C_{27}H_{26}O_2$	3	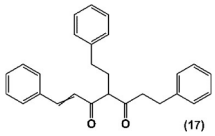 (17)
6.13	463.0905 [M-H]⁻	463.0876 [M-H]⁻	Isoquercetin **(18)**	$C_{21}H_{20}O_{12}$	4,5	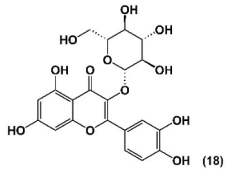 (18)
6.738	447.0958 [M-H]⁻	447.0927 [M-H]⁻	Quercitrin **(1)**	$C_{21}H_{20}O_{11}$	4,5	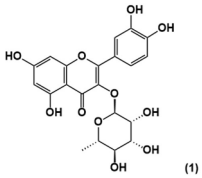 (1)
7.194	533.1860 [M-H]⁻	533.1870 [M-H]⁻	Isosyringinoside **(19)**	$C_{23}H_{34}O_{14}$	4,5	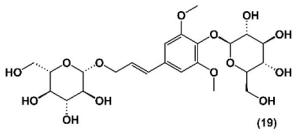 (19)
7.429	431.1013 [M-H]⁻	431.0978 [M-H]⁻	Apigetrin **(20)**	$C_{21}H_{20}O_{10}$	5	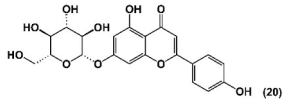 (20)

* FA: Formic acid.

mg (1.6 % m/m). HPLC-UV-MS analysis, configured for analytical scale samples, of the fractions indicated that the medium polar fraction (U2) was rich in quercitrin **(1)**, as shown in the negative ESI-mode BPI chromatogram in Fig. 6.

3.6. Isolation and characterisation of quercitrin *(1)* from the upscaled fraction

Isolation of 5.97 mg of the target compound, from upscaled fraction U2, was accomplished by repeat injections on the semi-preparative HPLC fractionation. UPLC-QTOF/MS analysis of this isolated fraction (F1) showed that it was 90.64 % pure, as shown in Fig. 7. The isolated quercitrin **(1)**, (an α-*l*-rhamnoside) aligned in both retention time (RT =

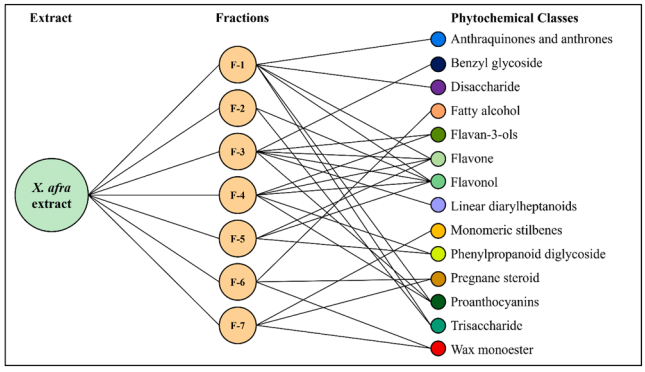

Fig. 4. Network depicting the distribution of phytochemical classes across the SPE fractions generated from the X. afra extract.

6.74 min) and accurate mass with that initially observed in the SPE Fraction 5 (from the small-scale extract). Its structure was confirmed through 1D- and 2D-NMR analysis.

Quercitrin (1): *m/z*([M+H]$^+$) = 449.1096 (neutral formula: $C_{21}H_{20}O_{11}$), Δm = −3.85 ppm (−1.72 mDa); ^{1}H-NMR (500 MHz, CD_3OD) δ (ppm): 7.34 (**H-1**, d, ^4J 2.21 Hz), 7.31 (**H-2**, dd, ^3J 8.29 Hz, ^4J 2.28 Hz), 6.91 (**H-3**, d, ^3J 8.46 Hz), 6.38 (**H-4**, d, ^4J 2.23 Hz), 6.21 (**H-5**, d, ^4J 2.23 Hz), 5.35 (**H-6**, d, ^3J 1.27 Hz), 4.22 (**H-7**, dd, ^3J 3.34 Hz, ^3J 1.59 Hz), 3.75 (**H-8**, dd, ^3J 9.23 Hz, ^3J 3.34 Hz), 3.42 (**H-9**, m), 3.34 (**H-10**, d, ^3J 9.71 Hz), 0.94 (**H-11$_3$**, d, ^3J 6.21 Hz). ^{13}C-NMR (500 MHz, CD_3OD) δ (ppm): 179.7 (**C-1**), 166.0 (**C-2**), 163.2 (**C-3**), 159.3 (**C-4**), 158.6 (**C-5**), 149.8 (**C-6**), 146.4 (**C-7**), 136.2 (**C-8**), 123.0 (**C-9**), 122.9 (**C-10**), 116.9 (**C-11**), 116.4 (**C-12**), 105.9 (**C-13**), 103.7 (Rha-**C-14**), 99.9 (**C-15**), 94.7 (**C-16**), 73.3 (Rha-**C-17**), 72.1 (Rha-**C-18**), 72.0 (Rha-**C-19**), 71.9 (Rha-**C-20**), 17.7 (**C-21**).

Detailed analysis of the configurations of the stereocentres of the carbohydrate moiety, confirmed to be L-rhamnose bound in the α-configuration to a quercetin aglycone, is provided for in the **Supplementary Information**. This confirmation of the identity of the isolated compound as quercitrin **(1)** adds to the very limited current knowledge of phytochemistry in *X. afra* as the presence of quercitrin **(1),** in the plant, has not previously been confirmed. Fig. 8.

3.7. Confirmation of antiplasmodial activity of quercitrin *(1)*

The dose-response model (n = 2) for quercitrin **(1)**, against BSF *P. falciparum* (3D7), indicated a mean IC_{50} (±SD) of 2.76 (±2.52) μM. The dose-response model is shown in Fig. 9. Compared to the commercial antiplasmodial, mefloquine (also the study positive control – IC_{50} = 30–60 nM), quercitrin **(1)** exhibits moderate antiplasmodial activity against this CQs strain. This moderate activity against

Table 5
Quercitrin antiplasmodial IC_{50}-values as indicated in literature.

P. falciparum strain	IC_{50} – μM (μg/mL)	Source
CDC1	9.1 (4.1)	Liu et al., 2007
3D7*	13.3 (5.96)	Zofou et al., 2013
Dd2*	5.0 (2.26)	Zofou et al., 2013
FcB1	71.4 (32.0)	Tajuddeen et al., 2021
3D7	>40 (>89.2)	Robertson et al., 2017
Dd2	>40 (89.2)	Robertson et al., 2017
K1	11.67 (5.23)	Ganesh et al., 2012

* The assays in Zofou et al. (2013) were done by measuring parasite lactose dehydrogenase activity.

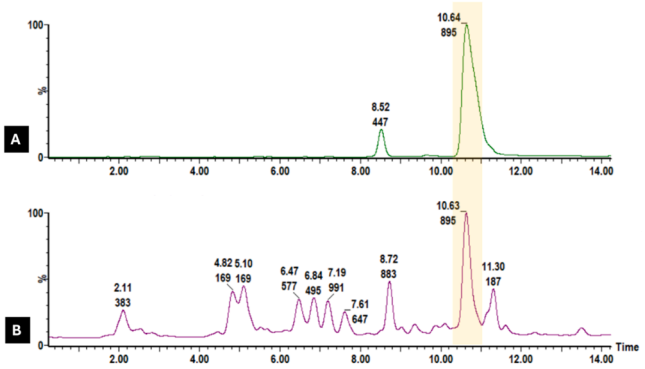

Fig. 6. Negative ESI-mode chromatograms from the analytical scale HPLC-MS analysis of the quercitrin (1) rich SPE fraction (U2): (A) extracted ion chromatogram for *m/z* = 447 ([M-H]- ion of (1)), (B) base peak ion (BPI) chromatogram of SPE fraction U2.

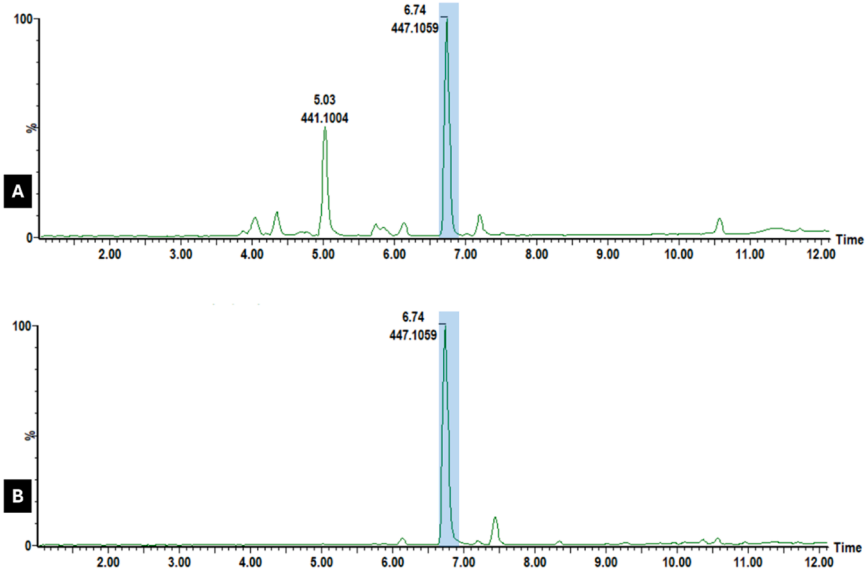

Fig. 5. ESI-negative mode mass-chromatograms (BPI) of (*A) spe* fraction 4 and (B) SPE fraction 5 from the extract of X. afra. The compound targeted for isolation, which is also the major compound in fraction 5, is highlighted in blue at retention time 6.74 min.

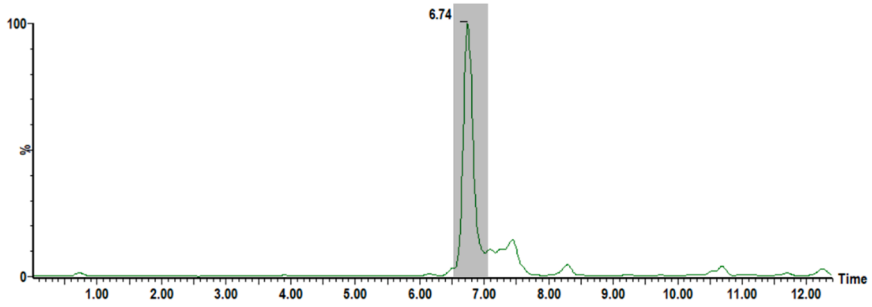

Fig. 7. A UPLC-QTOF/MS BPI chromatogram, in the negative ESI-mode, of the isolated semi-preparative HPLC fraction, with quercitrin (1) shaded in grey.

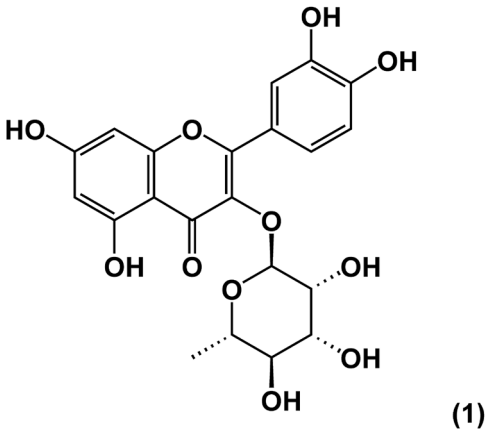

Fig. 8. Structure of quercitrin (1), as elucidated by NMR-analysis, confirming the tentative identity assigned to the major constituent of the potent antiplasmodial fractions.

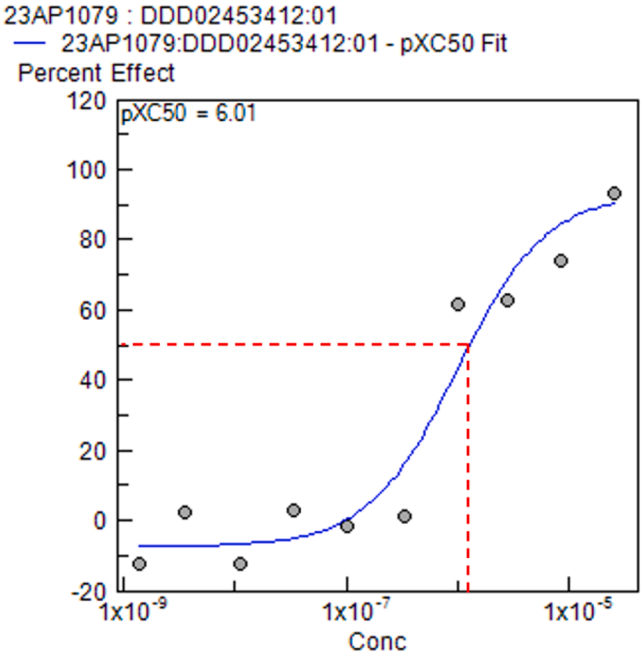

Fig. 9. Dose-response model of quercitrin (1) against P. falciparum (3D7) with the interpolation lines (red dashes) indicating an IC50 just over 1 μM.

P. falciparum (3D7), not yet reported for quercitrin **(1)**, correlated well with the trend observed in recent studies on flavonoid anti-malarial activity (Onisuru and Achilonu, 2025). Compounds in the classes of both flavanols and flavonols, as well as the associated glycoside derivatives, have been known to exhibit moderate *in vitro* antiplasmodial activity, with several showing promise as scaffolds for further drug development. This is detailed in the extensive review by Boniface and Ferreira (2019). This review also mentions several *in vitro* assay results of quercitrin **(1)**, against other strains of malaria, referencing Ganesh et al. (2012), where quercitrin **(1)** was found to have an IC_{50} of 11.67 μM against the chloroquine resistant (CQr) K1 strain of *P. falciparum* (K1). Other similar studies of the *in vitro* activity of quercitrin **(1)** were listed, together with the result from Ganesh et al. (2012), in Table 5.

Similarly, a very low toxicity was observed for **(1)** against rat skeletal myoblast cells (L6 cell line) where its IC_{50} was >200 μM (Tasdemir et al., 2006). Compared to the IC_{50} of quercitrin, measured in this study, a selectivity index (SI)>72.5. This low cytotoxicity makes quercitrin **(1)**, as with other flavonoids, ideal for investigation as lead compounds in antiplasmodial drug discovery, when viewed together with the associated moderate *in vitro* activity against *P. falciparum* (Onisuru and Achilonu, 2025). Detailed investigation into the structure-activity relationships would further improve understanding of modifications, to the flavonol glycoside structures, to later improve the antiplasmodial activity.

Compared with literature cited activity for **(1)** against *P. falciparum* (K1), its activity against the 3D7-strain is an improvement. The resistance index calculated relative to the *P. falciparum* 3D7-strain was 4.23, which is significantly different from the high resistance index of chloroquine for the same strains (RI = 40.0) (Agarwal et al., 2017). This was also observed by Ganesh et al. (2012). The favourable anti-malarial activity profile for quercitrin **(1)** prompted further investigation into the possible mode-of-action (MoA) by which it functions.

3.8. Investigating possible activity of quercitrin (1) against P. falciparum KRS1

The high *in vitro* activity of cladosporin, in inhibiting lysyl-tRNA-synthase (KRS1) in *P. falciparum*, has made it a promising lead in developing scaffolds for new anti-malarial drugs (Baragaña et al., 2019; Hoepfner et al., 2012).

The notable similarity between compounds cladosporin and quercitrin **(1)** was observed. Especially the tricyclic-polyphenol skeletons, as well as the presence of carbonyl groups orthogonal to the bicyclic part of the skeleton, supports the rationale for screening quercitrin **(1)** for possible inhibitory activity against KRS1. The assay, run in duplicate, showed compound **(1)** had no significant activity in inhibiting KRS1, across the full range of concentrations assayed. The response models for the assays are supplied in the **Supplementary Information**.

The stark difference in the level of KRS1-inhibition, between quercitrin **(1)** and cladosporin, could be due to subtle structural differences within the general tricyclic skeletons. Specifically, the oxygen atom arrangements in the fused bicyclic systems. The length and decreased flexibility of the side chain, as well as the steric hinderance from the hydrocarbon, on quercitrin **(1)** may have also negatively impacted the binding in the KRS1-active site.

Alternatively, the activity of quercitrin **(1)** against *P. falciparum* glutathione S-transferase (*Pf*GST) should also be considered for future work. This mode of action pathway, like the targeting of *Pf*KRS1, holds potential in reversing the damage done by chloroquine and ACT-resistance in malaria management. Some flavonoids have already been found to be active along this mode of action pathway (Onisuru and Achilonu, 2025). A study by Onisuru &Achilonu (2025) investigated this potential for 506 flavonoids *in silico*, followed by *in vitro* verification of the predicted active compounds, and found several flavonoids were potent *Pf*GST-inhibitors.

3.9. *In vitro trypanocidal activity of quercitrin (1)*

In contrast to its moderate antiplasmodial activity, quercitrin **(1)** did not exhibit any measurable activity against BSF *T. b. brucei* (Lister strain 427). In developing a dose-response model, for trypanocidal activity, it was not possible to obtain 50 %-inhibitory effect against the *Trypanosoma* parasites, within the assayed concentration range, as shown in Fig. 10. A similar result was observed when quercitrin **(1)** was assayed against *T. b. rhodesiense* (causative parasite of East African HAT) in which it was found to have an IC_{50} of 62 μM (Tasdemir et al., 2006), which is outside the range of the assay performed at the DDU.

Based on the activity of the initially screened SPE fractions the more complex fractions, neighbouring the semi-pure quercitrin **(1)** of fraction 5, showed more potent trypanocidal activity. Since quercitrin **(1)** was also present in these fractions, this could point to possible synergism between quercitrin **(1)** and the other flavonoids and proanthocyanidins in these fractions. This is supported by the observations of Tasdemir et al. (2006), regarding the trypanocidal activity of flavonoids and proanthocyanidins.

4. Conclusion

Through rapid bioactivity guided fractionation and advanced chromatographic isolation techniques, this study was successful in isolating quercitrin **(1)**, confirmed via NMR analysis, as the principal antiplasmodial constituent of *X. afra* leaves. Its moderate activity was similar to a previously reported potency determined through a different assay method (lactose dehydrogenase activity monitoring). In evaluating its potential use in treating HAT, the extract and fractions thereof were screened against *T. b. brucei* (Lister strain 427). In contrast to the moderate activity observed against *T. b. brucei*, the much less potent activity of quercitrin **(1)** was, as per literature, likely due to hinderance around the chalcone sidechain. Nonetheless, the *in vitro* activity of *X. afra* against *T. brucei* parasites has been confirmed and, through screening of the individual fractions of the extract, assigned to the flavonol, flavone, and proanthocyanidin constituents thereof. This work has, therefore, has gone to further studies than other reported studies in not only determining *in vitro* activity of an extract and semi-purified fractions of *X. afra*, but also included isolation of an active antiplasmodial compound from the plant material. Quercitrin **(1)**, the isolated compound, was also assayed in an MoA-study against *Pf*KRS1, where it was found to have no significant inhibitory effect.

The complexity and cost of *in vivo* assays forces careful consideration prior to commencement. Prospective future work, building on the *in vitro* results would firstly include optimisation of the bioactivity of quercitrin **(1)** through the synthesis of *in silico* designed derivatives. Once sufficient potency is obtained *in vitro* against the parasite, can toxicity studies and *in vivo* studies considered. Additionally, attention ought to be given to further elucidation of the mode of action associated with the antiplasmodial activity of quercitrin **(1)**. Likewise, the potential of synergistic trypanocidal relationships between the flavonoids should also be investigated, as this may guide possible formulations of complementary medicine which could shorten HAT-treatment regimens.

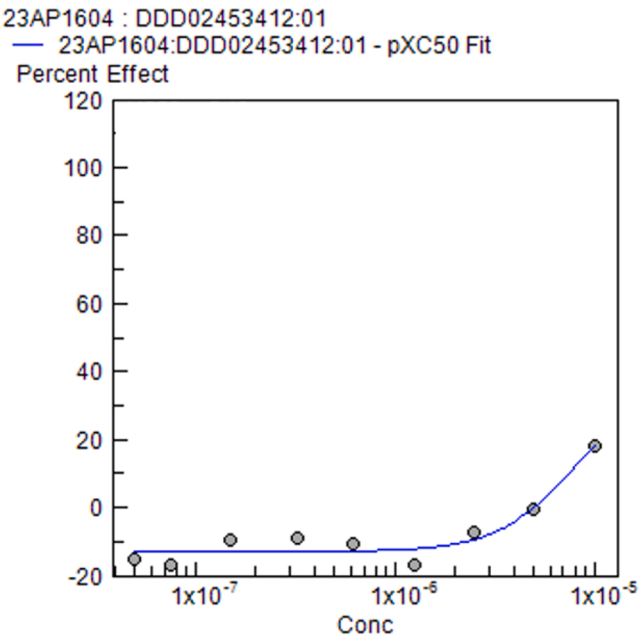

Fig. 10. Dose-response curve for quercitrin (1), isolated from X. afra, against BSF T. b. brucei (strain 427). Figure supplied by DDU at University of Dundee.

Funding sources

This project was done with the aid of funding for the Biodiscovery Centre, received from the Department of Science and Innovation, Republic of South Africa.

CRediT authorship contribution statement

Wiehan Rudolph: Writing – original draft, Validation, Methodology, Investigation, Formal analysis, Data curation. **Lauren Webster:** Supervision, Methodology, Formal analysis. **Cedric Graebin:** Methodology, Investigation, Formal analysis. **Vinesh Maharaj:** Writing – review & editing, Supervision, Resources, Project administration, Formal analysis, Conceptualization.

Declaration of competing interest

The authors declare that they have no known competing financial interests or personal relationships that could have appeared to influence the work reported in this paper.

Acknowledgements

The authors would like to acknowledge the contributions of Dr Madelien Wooding, the manager and principal operator at the LC-MS Synapt Facility at the University of Pretoria. Thank you also to Dr Olusola Bodede for insights in the elucidation of the compound structure from the NMR and MS data, also to Mr. Luke Invernizzi, Mr. Patrick McMillan, Dr Mamoalosi Selepe, and Dr Phanankhosi Moyo for your guidance and the training provided. To all the members of the Biodiscovery Centre, thank you. In his absence, a special thank you to Mr. Dilip Jagjivan, from UKZN, for remote assistance in optimisation of the quality of NMR spectroscopy. A very special gratitude to the WCAIR division and the Drug Discovery Unit at the University of Dundee for conducting our biological assays.

Supplementary materials

Supplementary material associated with this article can be found, in

the online version, at doi:10.1016/j.sajb.2025.08.037.

References

Agarwal, P., et al., 2017. *Vitro* susceptibility of indian plasmodium falciparum isolates to different antimalarial drugs & antibiotics. Indian J. Med. Res. 146 (5), 622–628. https://doi.org/10.4103/ijmr.IJMR_1688_15.

Baker, N., et al., 2013. Drug resistance in African trypanosomiasis: the melarsoprol and pentamidine story. Trends. Parasitol. 29 (3), 110–118. https://doi.org/10.1016/j.pt.2012.12.005.

Baragaña, B., et al., 2019. Lysyl-Trna Synthetase as a drug target in malaria and cryptosporidiosis. Proc. Natl. Acad. Sci. 116 (14), 7015–7020. https://doi.org/10.1073/pnas.1814685116.

Boniface, P.K., Ferreira, E.I., 2019. Flavonoids as efficient scaffolds: recent trends for malaria, leishmaniasis, Chagas disease, and dengue. PhytOther Res. 33 (10), 2473–2517. https://doi.org/10.1002/ptr.6383.

CDC, 2019. Trypanosomiasis, African [online]. https://www.cdc.gov/dpdx/trypanosomiasisafrican/index.html. (Accessed 2025-04-21).

CDC, 2020. Parasites - African trypanosomiasis (Also Known as Sleeping Sickness) [online]. https://www.cdc.gov/parasites/sleepingsickness/disease.html. (Accessed 2023-06-08).

Clarkson, C., et al., 2004. *In vitro* antiplasmodial activity of medicinal plants native to or naturalised in South Africa. J. Ethnopharmacol. 92 (2–3), 177–191. https://doi.org/10.1016/j.jep.2004.02.011.

Fola, A.A., et al., 2023. Clonal spread of *plasmodium falciparum* candidate Artemisinin partial resistance *Kelch13* 622i mutation and Co-occurrence with *Pfhrp2/3* deletions in Ethiopia. medRxiv. https://doi.org/10.1101/2023.03.02.23286711, 2023.2003.2002.23286711.

Fotie, J., 2008. The antiprotozoan potential of flavonoids. Pharmacogn. Rev. 2 (3), 6–19. DOI: None.

Frearson, J.A., et al., 2010. *N*-myristoyltransferase inhibitors as new leads to treat sleeping sickness. Nature 464 (7289), 728–732. https://doi.org/10.1038/nature08893.

Ganesh, D., et al., 2012. Antiplasmodial activity of flavonol quercetin and its analogues in plasmodium falciparum: evidence from clinical isolates in Bangladesh and standardized parasite clones. Parasitol. Res. 110 (6), 2289–2295. https://doi.org/10.1007/s00436-011-2763-z.

Gunn, A., Pitt, S.J., 2012. 2.7.3 Genus *Trypanosoma*, Parasitology - an Integrated Approach. John Wiley & Sons, Ltd, Hoboken, NJ, USA, pp. 70–81.

Hoepfner, D., et al., 2012. Selective and specific inhibition of the plasmodium falciparum lysyl-trna synthetase by the fungal secondary metabolite cladosporin. Cell Host. Microbe 11 (6), 654–663. https://doi.org/10.1016/j.chom.2012.04.015.

Hutchings, A., et al., 1996. Zulu Medicinal Plants - an Inventory. University of Natal Press, Scottsville, KwaZulu-Natal, South Africa.

Ismail, F.M.D., et al., 2020. Chapter four - antiparasitic natural products. In: Sarker, S.D., Nahar, L. (Eds.), Annual Reports in Medicinal Chemistry. Academic Press, pp. 115–151.

Iwu, M.M., 2014. Catalog of Major African Medicinal Plants, Handbook of African Medicinal Plants. Taylor & Francis Group, Boca Raton, Florida, USA, pp. 7–109. LLC.

Jacob, A., et al., 2021. A comparative assessment of the phytochemical composition of *Ximenia Caffra* (Sour Plum) leaf. Arab. J. Chem. Environ. Res. 8 (02), 418–435. DOI: None.

Kim, S., et al., 2023. Pubchem 2023 update. Nucleic. Acids. Res. 51 (D1), D1373–D1380. https://doi.org/10.1093/nar/gkac956.

Kuepfer, I., et al., 2011. Clinical presentation of T.B. Rhodesiense sleeping sickness in second stage patients from Tanzania and Uganda. PLoS. Negl. Trop. Dis. 5 (3), e968. https://doi.org/10.1371/journal.pntd.0000968.

Larit, F., et al., 2021. Proposed mechanism for the antitrypanosomal activity of quercetin and myricetin isolated from Hypericum Afrum Lam.: phytochemistry, *in Vitro* testing and modeling studies. Molecules 26 (4), 1009. https://doi.org/10.3390/molecules26041009.

Liu, Y., et al., 2007. Antimalarial flavonol glycosides from Euphorbia Hirta. Pharm. Biol. 45 (4), 278–281. https://doi.org/10.1080/13880200701214748.

Maluleke, M.K., et al., 2024. Exploring the biochemical constituents, medicinal properties and potential commercialization of Ximenia Caffra Sond. For enhancing Human health: a comprehensive review. Discov. Appl. Sci. 6 (1), 21. https://doi.org/10.1007/s42452-024-05639-1.

Maroyi, A., 2016. Ximenia Caffra Sond.(Ximeniaceae) in Sub-Saharan Africa: a synthesis and review of its medicinal potential. J. Ethnopharmacol. 184, 81–100. https://doi.org/10.1016/j.jep.2016.02.052.

MMV, 2023a. 5 Species of *plasmodium* parasites [online]. https://www.mmv.org/malaria/5-species-plasmodium-parasites. (Accessed 2023-06-08).

MMV, 2023b Malaria symptoms and treatment options [online]. https://www.mmv.org/malaria/about-malaria/malaria-symptoms-and-treatment-options. (Accessed 2025-03-19).

Ndong Ngomo, J.M., et al., 2023. Drug resistance molecular markers of Plasmodium falciparum and severity of malaria in Febrile children in the sentinel site for malaria surveillance of melen in Gabon: additional data from the Plasmodium Diversity Network African Network. Trop. Med. Infect. Dis. 8 (4), 184. https://doi.org/10.3390/tropicalmed8040184.

Nerima, B., et al., 2007. Detection of mutant P2 adenosine transporter (Tbat1) gene in Trypanosoma Brucei Gambiense isolates from Northwest Uganda using Allele-specific polymerase chain reaction. Trop. Med. Int. Health 12 (11), 1361–1368. https://doi.org/10.1111/j.1365-3156.2007.01918.x.

Norcross, N.R., et al., 2016. Trisubstituted pyrimidines as efficacious and fast-acting antimalarials. J. Med. Chem. 59 (13), 6101–6120. https://doi.org/10.1021/acs.jmedchem.6b00028.

Onisuru, O., Achilonu, I., 2025. High-throughput virtual screening and empirical validation of probable inhibitors of plasmodium falciparum and vivax glutathione transferase using bromosulfophthalein as the benchmark Ligand. Int. J. Biol. Macromol. 302, 140526. https://doi.org/10.1016/j.ijbiomac.2025.140526.

Peacock, L., Ferris, V., Bailey, M., Gibson, W., 2008. Fly transmission and mating of Trypanosoma brucei brucei strain 427. Mol. Biochem. Parasitol. 160, 100–106. https://doi.org/10.1016/j.molbiopara.2008.04.009.

Robertson, L.P., et al., 2017. Pimentelamines a–C, indole alkaloids isolated from the leaves of the australian tree Flindersia Pimenteliana. J. Nat. Prod. 80 (12), 3211–3217. https://doi.org/10.1021/acs.jnatprod.7b00587.

Rutz, A., et al., 2022. The lotus initiative for open knowledge management in natural products research. Elife 11, e70780. https://doi.org/10.7554/eLife.70780.

Soré, H., et al., 2018. Antiplasmodial properties of plants isolated flavonoids and their derivatives. Int. J. Herb. Med. 6 (5), 43–56. DOI: None.

Tajuddeen, N., et al., 2021. Antiplasmodial and cytotoxic activities of extract and compounds from Ozoroa Obovata (Oliv.) R. & A. Fern. Var. Obovata. Chem. Biodivers. 18 (8), e2100240. https://doi.org/10.1002/cbdv.202100240.

Tasdemir, D., et al., 2006. Antitrypanosomal and antileishmanial activities of flavonoids and their analogues: *in vitro, in vivo*, structure-activity relationship, and quantitative structure-activity relationship studies. Antimicrob. Agents Chemother 50 (4), 1352–1364. https://doi.org/10.1128/AAC.50.4.1352-1364.2006.

Thornburg, C.C., et al., 2018. Nci Program for Natural Product discovery: a publicly-accessible library of Natural Product fractions for high-throughput screening. ACS. Chem. Biol. 13 (9), 2484–2497. https://doi.org/10.1021/acschembio.8b00389.

van Wyk, B.-E., Gericke, N., 2018. Women's Health, People's Plants - a Guide to Useful Plants of Southern Africa. Briza Publications, Pretoria, South Africa, pp. 215–234.

Vergara, S., et al., 2022. *In vitro* antiplasmodial activity of selected plants from the Colombian North Coast with low cytotoxicity. Trop. Parasitol. 12 (2), 78–86. https://doi.org/10.4103/tp.tp_9_22.

Watt, J.M., Breyer-Brandwijk, G., 1962. The Medicinal and Poisonous Plants of Southern and Eastern Africa; Being an Account of Their Medicinal and Other Uses Chemical Composition Pharmacological Effects and Toxicology in Man and Animal. E & S Livingstone Ltd, Edinburgh, Scotland.

WHO, 2024. Who guidelines for Malaria - 30 November 2024 [online]. https://app.magicapp.org/#/guideline/LwRMXj/section/j7DB3L. (Accessed 2025-03-19).

Zhen, J., et al., 2015. Phytochemical analysis and anti-inflammatory activity of the extracts of the African medicinal plant Ximenia Caffra. J. Anal. Methods Chem. 2015 (1), 948262. https://doi.org/10.1155/2015/948262.

Zofou, D., et al., 2013. New antimalarial hits from Dacryodes Edulis (Burseraceae) - part I: isolation, *in vitro* activity, in Silico "drug-likeness" and pharmacokinetic profiles. PLoS. One 8 (11), e79544. https://doi.org/10.1371/journal.pone.0079544.

Zong, C.Y., Xian, Z., 2023. Natural product activity and species source database (NPASS), Ximenia Afra [online]. https://bidd.group/NPASS/search_organism.php. (Accessed 2025-07-19).